

The Interstellar Bullet Engine IRAS 05506+2414

Nicholas W. Stantzos¹ and Raghvendra Sahai²

Jet Propulsion Laboratory, California Institute of Technology, Pasadena, CA, 91109

Throughout their life-cycles, high-mass stars inject large amounts of energy and momentum into their environments through stellar winds. Results from a study of the Orion BN/KL region indicate that disruption of a massive young stellar system can lead to an explosive event producing a wide-angle outflow, different from the classical bipolar flows driven by young stellar object (YSO) accretion disks. The discovery of a massive YSO, IRAS 05506+2414, may prove to be the second instance of this uncommon outflow. Prior to this study, data was collected using the Arizona Radio Observatory's 10-meter and 12-meter telescopes. Spectra of 16 different molecular line transitions were organized, reduced, and prepared for further analysis. A variety of molecular transitions were observed, such as 12CO 2-1, HCO+ 3-2, CS 3-2, in order to probe physical conditions of the YSO. From line transitions like HCO+ 3-2, we will determine physical properties like density, temperature, and velocity of our source object. For each molecular transition, the spectra were averaged in subsets, which were then averaged to produce a final spectra with an optimal signal to noise ratio. Future radiative modeling will yield mass and energetics of IRAS05506+2414.

I. Introduction

Young stellar objects (YSOs) are classified as young stars in their early evolutionary sequence. YSOs have evolved past the protostar phase, though have not made it to the main sequence. YSOs are commonly associated with bipolar outflows, polar jets, and proto-planetary disks. During a previous survey of multi-wavelength pre-planetary nebulae (PPN) survey (Sahai et al. 2008), a serendipitous discovery of an energetic outflow source IRAS 05506+2414 was made. Sahai et al. 2008 provide evidence though their survey that supports IRAS 05506+2414 as likely being a massive star. The purpose of this paper is to investigate the nature of massive young stars and their volatile life cycles. Specifically, we want to know if the object IRAS05506+2414 has at its center a massive star undergoing an explosive event that is producing a wide-angle outflow. This phenomenon, if it is occurring, is completely different from the classical bipolar outflows that are typical in the evolution of young stellar objects.

What causes these explosive wide angle outflows to occur? In answering this question, another problem will be inherently resolved. The same explosive event was observed in the well-studied Orion BN/KL region, and speculations have been made on the uniqueness of this occurrence in young massive stars. This project aims to shed light on the nature of IRAS05506+2414 and thereby provide a better understanding of the wide angle outflow in the Orion BN/KL region. This question arose as optical images of IRAS05506 were taken with the Hubble Space Telescope (HST) and this phenomenon was discovered. Our solution would provide robust confirmation to speculations we have made about the nature behind the observed phenomena. Not only would we gain insight into IRAS05506, we would also be able to make conclusions on the events taking place in the Orion BN/KL region, and determine the rarity of such outflows.

Molecular line spectra are useful in probing physical and chemical properties of sources like IRAS 05506+2414. Physical and chemical properties such as temperature, density, and molecular abundance are able to be constrained through analysis and Gaussian fitting of the line intensities of the observed spectra. Line intensities of each spectra are able to provide specific energetics of the observed molecular transition, which translate to each of the properties mentioned earlier. Subsequent analysis of molecular line data on this outflow source, data reduction and calibration with the software package CLASS/GILDAS will yield important information about the physical and chemical conditions of the cloud surrounding, and the outflow emanating from IRAS05506. This data reduction will provide us with precision in knowing the energetics and mass of the outflow, which will bring us ever closer to complete understanding of this enigmatic stellar outflow of IRAS05506.

¹ USRP Intern, Astrophysics and Space Science, JPL.

² Principal Research Scientist, Astrophysics and Space Science, 183-900, JPL.

II. Observations

Observations were made using the Arizona Radio Observatory's 12 Meter (12M) and Submillimeter Telescope (SMT) at millimeter and sub-millimeter wavelengths, respectively. Approximately 1450 useable spectra were gathered throughout 12 non-consecutive nights of observing our source. All of the observations were made in November of 2007, January 2008, and February 2008. 9 different molecules were observed, each with multiple transitions as listed in Table 1 below. Spectra were taken towards our source, and the surrounding cloud to produce a map of the emission in the ^{12}CO and ^{13}CO $J=1-0$ and $2-1$ transitions.

Molecule	Transition	Frequency
HCO+	J=1-0	89188.53
HCO+	J=3-2	267557.63
C18O	J=1-0	109782.16
^{13}CO	J=1-0	110201.35
^{13}CO	J=2-1	220398.69
^{12}CO	J=1-0	115271.20
^{12}CO	J=2-1	230537.99
^{12}CO	J=3-2	345795.96
SiO	J=3-2	130268.72
SiO	J=6-5	260518.08
SO	J,K=3,4-2,3	138178.68
SO	J,K=6,5-5,4	251825.82
SO	J,K=6,7-5,6	261843.76
SO ₂	J,K=4(2,2)-4(1,3)	146605.51
SO ₂	J,K=11(1,11)-10(0,10)	221965.20
SO ₂	J,K=4(3,1)-4(2,2)	255553.29
CS	J=3-2	146969.05
H ₂ CO	J,K=2(1,1)-1(1,0)	150498.34

Table 1: List of molecules, transitions, and frequencies observed.

III. Data Reduction

To reduce and analyze the collected spectra, the program Continuum and Line Analysis Single-dish Software (CLASS) was utilized. This GILDAS software is capable of simple organizational techniques, along with reduction methods like averaging, baseline subtractions, and Gaussian fits. Though CLASS's capability far exceeds these techniques listed, the data reduction procedures only made use of the aforementioned methods.

In order to obtain the maximum signal to noise ratio, simple averaging techniques were employed upon the 1450 useable spectra. Due to the vast quantity of data being handled, many scripts were created to perform reduction methods (averaging, baseline subtractions, production of post scripts) on the spectra and aid in the reduction process. Data for any particular molecular line are obtained by observing the source over an extended period of time which can last several hours. However because of possible changes in the observing condition (e.g., receiver sensitivity, clouds, telescope pointing depth), spectra are recorded every few minutes. In order to check for such changes which will affect the line intensity, I produced sub-averages of typically 3-4 spectra, which were then combined into a final

average after inspection. Before any averaging took place, spectra was sorted by transition, offset, and acquiring telescope Figure 1 (following page) shows a single spectra, before any data reduction processes were applied.

A. Non-mapping observations

Averages were only done on spectra of the same transitions, at the same offset, and taken with the same telescope. The majority of the spectra (non-mapping spectra) were taken while the telescope was centered on the source, with no offset. After the spectra were grouped by transition and telescope, they were arranged into subsets, depending on their individual rms values. By making subsets with similar rms values, we assured that the signal to noise ratio was not affected by any single spectra that might have anomalously large noise levels. In addition to boosting the signal to noise ratio, this technique improved the baseline of the average of each subset (subaverage). Baseline subtractions are important if one wishes to attain an accurate peak intensity measurement. Baseline subtractions compensate for any intensity offsets a spectra might have, in other words, if a spectra's baseline is roughly centered around 1.0 on the y axis, instead of 0, then a baseline subtraction will center the baseline at zero, providing for more certainty when obtaining peak intensities. This technique essentially is the subtraction of instrumental or atmospheric signal using a linear baseline where emission from the cloud is not present. The area subtracted has no astrophysical significance, so the signal is not affected.

This process of making subaverages was then repeated, to create averages of the subaverages (superaverages). For the SMT, these superaverages are the final product of the data reduction, though some more steps are required for the 12M telescope. Every observation made with the 12M telescope yielded two spectra.

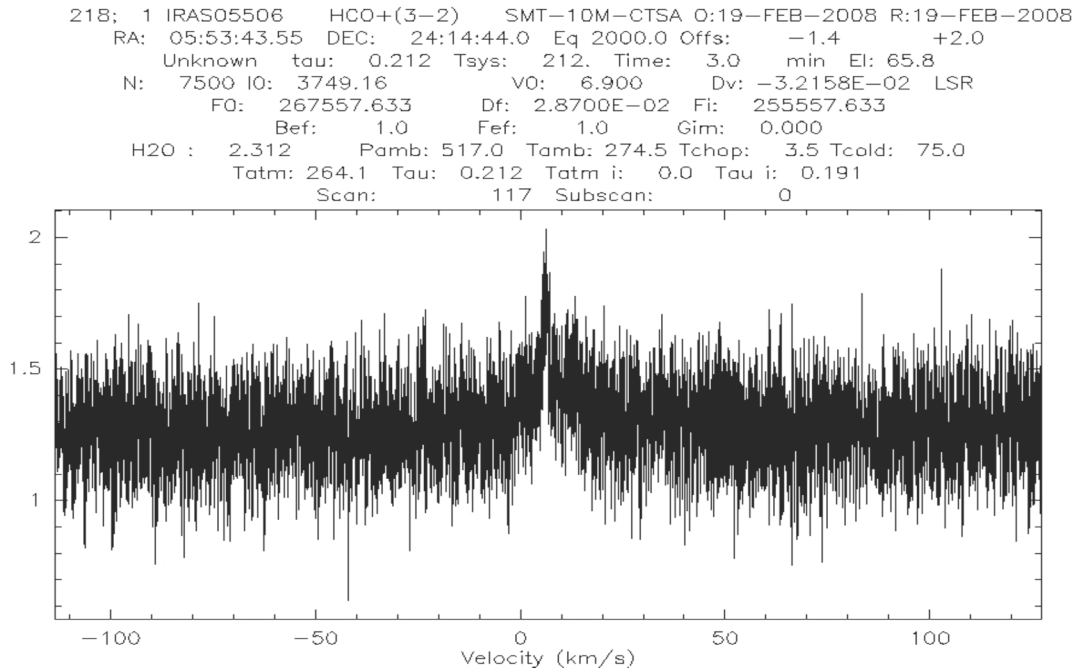


Figure 1: An HCO+ 3-2 spectrum from one observation with no baseline subtractions, or averaging. Notice how the baseline (signal-free region on the velocity axis) is not centered at an intensity of 0.

Figure 2 (following page) shows a superaveraged spectrum of a HCO+ 3-2 transition line.

B. Mapping observations

The rest of the observations (mapping observations) were made within a range of positions offset from the center of our source. These offset positions ranged anywhere from 180 to 1080 arcsecond offset from our source's center. With observations made in different positions, it is important to sort mapping spectra by their offset. There were a wide variety of offsets observed, so only a few observations per offset were made. Due to the fact that the outflow source IRAS05506+2414 is embedded in an extended interstellar molecular cloud, we needed to do these mapping observations to better characterize the environment of the outflow. The mapping spectra were individually analyzed. The spectra were put into a list, where they had baseline subtractions applied and were written to a separate file.

Upon writing them to another file, I examined each offset group and made a note of the individual peak intensities. The purpose of this was to compare peak intensities of spectra of the same line, taken at the same offset location. If the intensities were within 30% of each other, then they were safe to average. A result of the mapping observations was to obtain an accurate map of the 12CO and 13CO emission from the cloud, which will provide for more accurate estimates of the total cloud mass. As the number of offset positions were quite numerous, the corresponding averages were quite numerous as well. After the offset sorting and intensity comparisons were completed, the process which was used when averaging the non-mapping observations was used once again with the mapping observations.

```
2; 3 IRAS05506 HCO+(3-2) SMT-10M-CTSA O:19-FEB-2008 R:30-MAR-2011
RA: 05:53:43.55 DEC: 24:14:44.0 Eq 2000.0 Offs: -1.1 +2.2
Unknown tau: 0.213 Tsys: 209. Time: 70. min El: 71.3
N: 6256 l0: 2507.84 v0: -13.10 Dv: 3.2158E-02 LSR
FD: 267557.633 Df: -2.8700E-02 Fi: 255557.633
Bef: 1.0 Fef: 1.0 Gim: 0.000
H2O : 2.313 Pamb: 515.4 Tamb: 273.5 Tchop: 3.1 Tcold: 75.0
Tatm: 262.8 Tau: 0.213 Tatm i: 0.0 Tau i: 0.191
110- 124, 127- 134,
```

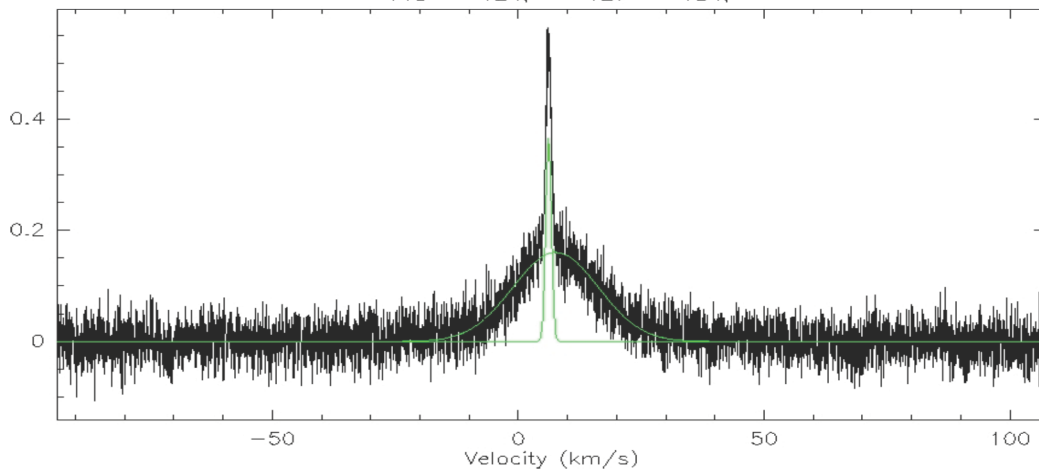


Figure 2: A complete superaverage of HCO+ 3-2 with a fitted Gaussian line. The broad component is the lower portion of the spectrum, while the narrow component is the upper, thinner peak.

IV. Analysis

A. Gaussian fits

Once all of the spectra were averaged to have the highest possible signal to noise ratio, Gaussian lines were fitted to these spectra. For each superaverage that was produced, Gaussian fitting techniques were used, and results were tabulated.

As mentioned before, the CLASS program has a built in Gaussian fit feature that only requires the user to identify the broad and narrow components of the spectral profile being fitted. The broad component of a spectrum is the lower, wider curve part of the spectrum, while the narrow component is the narrow spike directly above the broad component, an example being the HCO+ 3-2 spectrum in Figure 2. Gaussian lines were fit to each spectra that had a signal sufficiently larger than the noise present. Table 2 (below) shows a table of fit results from superaveraged spectra taken by the SMT. In Table 2 (below), the RMS, area, peak intensity, position, and line width are recorded, with the error bars being underneath in . parentheses. These values were used later in radiative transfer modeling. The spectra taken with the SMT did not already have beam efficiency correction applied, so this correction was applied prior to using these values prior to the radiative transfer modeling of the data.

NASA USRP – Internship Final Report

TELE: 12M

Obs	Mol.	Transition	Frequency	Shape	Rms	Area1 (Error)	Area2 (Error)	TA1* (K)	TA2* (K)	V1 (km/s) Error	V2 (kms/s) Error	Width1 (km/s) Error	Width2 (kms/s) Error	Epoch
9	12CO	1-0	115271.20	narrow	6.856E-02	23.48 (0.056)		5.44		6.27 (0.005)		4.05 (0.012)		nov-07
10	13CO	1-0	110201.35	narrow	2.870E-02	5.10 (0.015)		3.2604		6.308 (0.002)		1.470 (0.005)		nov-07
3	C18O	1-0	109782.16	narrow	2.620E-02	0.54 (0.011)		0.52		6.16 (0.009)		0.98 (0.024)		nov-07
11	HCO+	1-0	89188.53	narrow	4.604E-02	0.63 (0.030)		0.31		6.561 (0.042)		1.918 (0.118)		nov-07
4	S0	3,4-2,3	138178.68	narrow+broad	1.444E-02	0.15 (0.006)	0.32 (0.025)	0.16	0.02	6.22 (0.014)	8.05 (0.599)	0.91 (0.044)	17.6 (2.230)	nov-07
7	S0	4,3-3,2	158971.85	weak broad	1.576E-02		0.23 (0.017)		0.02		7.03 (0.368)		10.1 (0.866)	Feb-08
6	S02	4(2,2)-4(1,3)	146605.51	2.971E-02									jan-08
1	Si0	3-2	130268.72	2.516E-02									Feb-08
2	CS	3-2	146969.05	narrow	2.656E-02	0.20 (0.008)		0.22		6.256 (0.017)		0.854 (0.044)		nov-07
5	H2CO	2(1,1)-1(1,0)	150498.34	narrow	1.541E-02	0.31 (0.006)		0.27		6.24 (0.009)		1.08 (0.023)		jan-08

Notes:
1 is narrow velocity component
2 is broad velocity component

TELE: SMT-10M-CTSA

Obs	Mol.	Transition	Frequency	Shape	Rms	Area1 (Error)	Area2 (Error)	TA1* (K)	TA2* (K)	V1 (km/s) Error	V2 (kms/s) Error	Width1 (km/s) Error	Width2 (kms/s) Error	Epoch
12	12CO	2-1	230537.99	narrow+broad	3.509E-02	3.54 (0.016)	16.39 (0.035)	3.40	2.21	7.23 (0.002)	5.81 (0.007)	0.98 (0.004)	6.96 (0.017)	Feb-08
8	12CO	2-1[b]	230537.99	narrow+broad	3.193E-02	3.63 (0.018)	12.3 (0.036)	2.99	1.59	6.51 (0.002)	7.76 (0.010)	1.14 (0.005)	7.28 (0.026)	Feb-08
11	12CO	2-1[b]	230537.99	narrow+broad	0.223	3.58 (0.023)	16.5 (0.049)	3.25	2.13	-181.3[a] (0.002)	-179.9[a] (0.011)	1.03 (0.006)	7.29 (0.026)	Jan-08
6	12CO	3-2[b]	345795.96	broad+narrow	0.296	2.11 (0.162)	5.7327 (0.266)	1.39	0.78	7.22 (0.032)	5.42 (0.161)	1.42 (0.101)	6.94 (0.246)	Feb-08
9	13CO	2-1[b]	220398.69	narrow	3.284E-02	5.1696 (0.013)		3.05		-172.2[a] (0.002)		1.59 (0.005)		Jan-08
2	HCO+	3-2	267557.63	narrow+broad	2.898E-02	0.53 (0.011)	3.51 (0.039)	0.37	0.16	6.15 (0.012)	7.59 (0.107)	1.34 (0.030)	20.6 (0.286)	Feb-08
10	S0	6,5-5,4[b]	251825.82	narrow+broad	2.149E-02	7.04E-02 (0.010)	0.70 (0.035)	0.06	0.02	-756.1[a] (0.053)	-759.5[a] (0.617)	1.12 (0.211)	26.9 (1.884)	Jan-08
4	S0	6,7-5,6[b]	261843.76	broad	2.743E-02		0.97 (0.034)		0.06		6.84 (0.252)		16.3 (0.784)	Feb-08
1	S02	11(1,11)-10(0,10)	221965.20	1.302E-02									Feb-08
3	S02	4(3,1)-4(2,2)	255553.29	2.333E-02									Feb-08
5	Si0	6-5	260518.08	9.072E-02									Feb-08

1 is narrow velocity component
2 is broad velocity component

[a] velocities are incorrect due to error in data header

[b]
observation 11 is incorrectly labeled as 13CO(2-1)
observation 8 is incorrectly labeled as 13CO(2-1)
observation 6 is labeled in class as CO(3-2)
observation 9 is incorrectly labeled 12CO(2-1) in class
observation 10 is incorrectly labeled 12CO(2-1) in class
observation 4 is labeled S0(7-6) class

Table 2: Results from Gaussian fits done on superaveraged spectra taken by the 12M and SMT. Transitions with weak signal strength were not fitted with Gaussian functions. Note that TA= peak intensity, and V = position. 1 = narrow component, 2 = broad component.

1. Physical Properties

Both of the broad and narrow components of the spectrum contain information about the physical properties of

our source. The random motion of the cloud is represented by the velocity width of the narrow component. The CLASS software uses the observed frequency of the molecules, together with the doppler equation to calculate the shifted velocity, in this case the turbulent cloud motion. The velocity of the center of the narrow component represents the systemic velocity of the source.

The broad component represents the velocity of the outflow associated with IRAS 05506+2414. The width of the broad component represents twice the outflow speed, for example, since the width of the HCO+ 3-2 transition is approximately 20 km/s, the velocity in each direction (towards and away from the LSR) is about 10 km/s. We know that such large velocities must be associated with an outflow of some kind, since typical turbulent motions are only a few km/s.

The peak intensity is proportional to the column density of molecules emitting in that specific transition.

As with any Gaussian fit procedure, residual plots are made to determine the quality of the fit that was made. Every superaverage produced that had a reasonable signal strength was fitted with a Gaussian, and accompanying residual plots were made. One can attain confidence that the Gaussian fit was accurate if the residual plot of the fit is a flat line, containing only noise. For all of the line transitions, save 12CO 1-0, 2-1 and 13CO 1-0, 2-1, the residual plots were flat, and only containing noise. The specified 12CO and 13CO transitions did not have good Gaussian fits because those spectra do not form the shape of a Gaussian curve, due to the presence of a self absorption component. Figure 2, above, is a fine example of a spectrum containing Gaussian curves for the both the broad, and narrow components. Figure 3, below, is a residual plot made for the HCO+ 3-2 Gaussian fit.

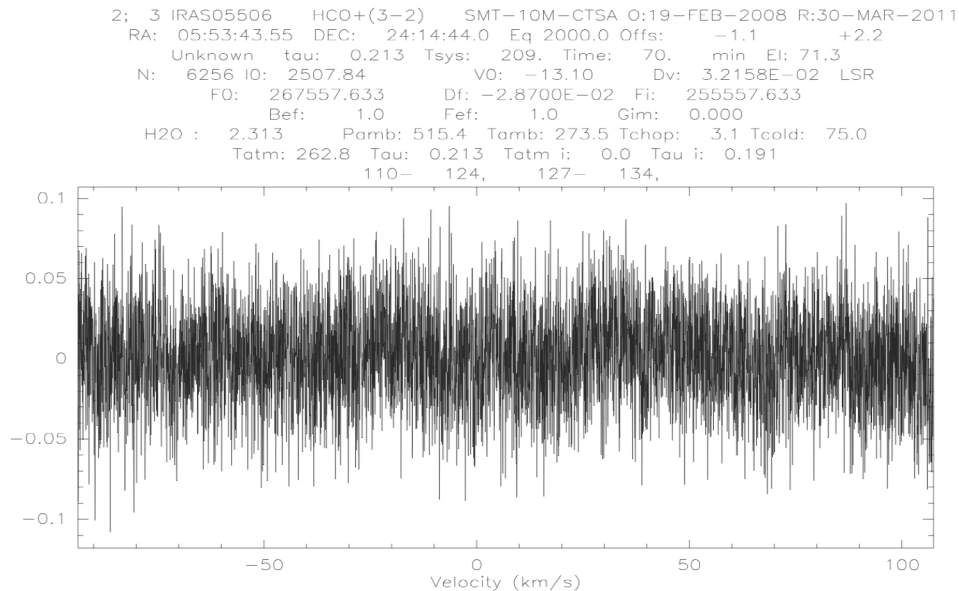


Figure 3: A residual plot made after the Gaussian fit was made for HCO+3-2. The absence of any identifiable shape or pattern indicates that the Gaussian fit technique was done correctly.

B. Radiative transfer modeling

After Gaussian fits were made and values were obtained, radiative transfer modeling immediately followed. Using the RADEX non-LTE molecular radiative transfer online tool for an isothermal homogeneous medium, we were able to place limits on the physical properties (density and kinetic temperature) of our observed source, IRAS 05506+2414. Table 3 (next page) is a conclusion of our modeling with RADEX. RADEX enables one to constrain specific molecular abundances and physical conditions (densities, temperature) from observations of molecular lines at millimeter and submillimeter wavelengths, by fitting our intensity and line widths for different molecules. We varied the kinetic temperature and number density, and found lower and upper limits on the density and kinetic temperature for different molecules. The cloud likely has strong gradients of density and temperature, with 12CO

tracing the regions with lowest density and temperature, and HCO+ and SO regions with the highest densities and temperatures.

Molecule	Transition	Kinetic temperature	Density	Tau
12CO	J=1-0	9.5K	>2e4	>2.3
	J=2-1			>4.1
	J=3-2			>2.2
13CO	J=1-0	11K	>4e5	>0.55
	J=2-1			>1.1
HCO+	J=1-0	13.5-25K	1e7-1e6	0.028-0.0013
	J=3-2			0.08-0.085
SO	J,K=3,4-2,3	9.5-25K	1.00E+07	0.028-0.0081
	J,K=6,5-5,4			0.0021-0.0049

Table 3: Result of RADEX modeling.

We were able to put more accurate constraints on the physical condition in the cloud using molecules with multiple transitions, i.e. 12CO, 13CO, HCO+, SO (Table 3). For the 12CO molecule for which 3 different transitions were observed, the physical conditions were most tightly constrained. This analysis demonstrates that strong gradients in density and temperature exist.

1. Parameters

Using our measured peak intensities, line widths, and a kinetic temperature derived using known 12CO transition data, we were able to estimate the cloud density and temperature, and column density of the observed molecular species.

The observed peak intensities for each molecular line is related to the excitation temperature and optical depth for that line via the radiative transfer equation:

$$T_R = T_{ex}(1 - e^{-\tau})$$

where Tau is optical depth (proportional to the column density of molecules along the observer’s line of sight), T_R is observed radiation temperature, T_{ex} is excitation temperature. For the 12CO line we can make the following approximation

$$\tau \gg 1 \qquad T_{ex} \approx T_K$$

This gives us the following result:

$$T_R \approx T_K$$

We derived a value of 9.5K for our kinetic temperature (T_K) of the cloud.

Well-constrained modeling could only be carried out for those molecules with multiple observed transitions, such as the 1-0 and 3-2 transitions of HCO+. Multiple intensity measurements for one molecule allow a ratio to be made between transitions, and this ratio between the transitions must be preserved when the modeling is done for an accurate result to be obtained. With only one transition, a molecule could have multiple values for different parameters and still produce the same radiation temperature.

For some molecules, the ratio of their transitions did not match up to the RADEX program's, under the given 9.5K kinetic temperature. The CO molecules make up the less dense extended cloud surrounding the source, with

densities lower than $4e5$. There are large gradients in density and temperature with the HCO⁺ and SO molecules, as these molecules have densities constrained from $1e7$ to $1e6$.

V. Conclusion and Future Work

Through the described process of data reduction, on-source spectra for 18 molecular transitions were produced with optimal signal to noise ratios. These spectra were then fitted with Gaussian functions, and the resultant line widths and peak intensities were then used in the RADEX radiative transfer program to determine bounds for densities and kinetic temperatures of the cloud associated with IRAS 05506+2414. Although this modeling is still in progress, we have placed upper and lower limits on the density, and kinetic temperature for the molecular source associated with the source IRAS 05506+2414. In addition, mapping spectra were subjected to similar data reduction methods, and averaged to produce a set of spectra with optimal signal to noise ratios. These spectra provide crucial information on the mass of the extended cloud in which the outflow source is embedded.

Utilizing these reduced molecular line transitions will enable us to build a complete physical model of IRAS 05506+2414, which will include for example, a central outflow source surrounded by an extended ambient cloud. Such a model will help answer questions regarding the unique nature of this outflow source.

Acknowledgments

This research was carried out at the Jet Propulsion Laboratory, California Institute of Technology and was sponsored by the Undergraduate Student Research Program (USRP) and the National Aeronautical and Space Administration

N.S. author thanks the USRA, the NASA USRP, Dr. Raghvendra Sahai, and Petra Kneissl-Milanian.

References

- ¹Sahai, R., Claussen, M., Contreras, C.S., Morris, M., and Geetanjali, S., “High Velocity Interstellar Bullets In IRAS 05506+2414: A Very Young Protostar,” *The Astrophysical Journal*, Vol. 680, Feb. 2008, pp. 483-494.
- ²Van der Tak, F.F.S., Black, J.H., Schöier, F.L., Jansen, D.J., van Dishoeck, E.F., 2007, *A&A* 468, 627-635.
- ³Hjalmarson, A., “Astrochemistry- Observational Aspects.” ESO-IRAM-ONSALA Workshop on (Sub)Millimeter Astronomy, June 1985